

Incompressible polaritons in a flat band

Matteo Biondi, Evert P. L. van Nieuwenburg, Gianni Blatter, Sebastian D. Huber, and Sebastian Schmidt
Institute for Theoretical Physics, ETH Zurich, 8093 Zürich, Switzerland

We study the interplay of geometric frustration and interactions in a non-equilibrium photonic lattice system exhibiting a polariton flat band as described by a variant of the Jaynes-Cummings-Hubbard model. We develop a semi-analytic projective method and employ an open system version of the time-evolving block decimation algorithm (TEBD) in order to calculate the non-equilibrium steady state of the array subject to drive and dissipation. We find that frustration strongly enhances photon repulsion in a flat band leading to an incompressible state of light. The latter manifests itself in strong spatial correlations, i.e., on-site and nearest-neighbor anti-bunching combined with extended density-wave oscillations at larger distances. We propose a state-of-the-art circuit QED realization of our system, which is tunable in-situ.

Over the last decade there has been a surge of interest in realizing strongly correlated states of light in interacting photonic lattices for quantum simulations and the study of non-equilibrium many-body physics [1–12] (for two recent reviews, see [13, 14]). Effective photon-photon interactions can be engineered in these systems utilizing strong light-matter couplings in various cavity/circuit QED platforms, e.g., with atoms [15], excitons [16, 17] or superconducting qubits [18, 19]. Arranging cavities and atoms/qubits on a lattice offers the opportunity to engineer strongly correlated states of photons in various geometries with local control over coherent as well as dissipative dynamics. The driven dissipative nature of photonic systems then allows for direct experimental, non-invasive access to the complete density matrix, e.g., temporal and spatial correlation functions [20].

A particularly challenging and interesting problem of many-body physics concerns the study of frustrated lattices. Frustration refers to the impossibility of satisfying simultaneously all constraints implied by a Hamiltonian, which are imposed, e.g., by geometry, disorder or interactions. This typically leads to macroscopically degenerate ground-states, which are sensitive to small perturbations and thus define a challenging minimization problem. Conversely, frustration often gives rise to interesting strongly correlated phenomena and the emergence of fascinating non-trivial structures, e.g., in quantum magnetism [21, 22], quantum hall systems [23–25], Josephson junctions [26, 27] or ultra-cold atoms [28–31]. In this work, we make use of geometric frustration to boost interactions and show that photons pumped into the flat band of a photonic lattice form an incompressible state of light with non-trivial spatial correlations at the onset of crystallization. This non-equilibrium steady state does not follow from energy minimization, but derives from a delicate balance of drive and dissipation.

First realizations of interacting photonic lattices have recently been engineered based on solid-state as well as semiconductor technologies [32–36]. Motivated by these achievements, we study a 1D qubit-cavity chain, where qubits couple to photons in every other cavity. Such a Jaynes-Cummings-Hubbard (JCH) system [1, 3, 37–46] is readily realizable with state-of-the-art circuit QED technology, where the lattice dispersion as well as the strength of the effective photon-photon interactions can be tuned in-situ by simply changing the qubit-resonator detuning [14]. We show that one of the Bloch bands

of the array can be tuned from dispersive to completely dispersiveless, i.e., flat in the entire Brillouin zone. This flat band arises due to destructive quantum interference and generates a macroscopic set of degenerate and localized plaquette states. Similar flat bands were recently observed in non-interacting 2D laser and micro-pillar arrays [34, 47].

Here, we investigate the effects of strong photonic interactions in such a non-equilibrium geometrically-frustrated system by using projective methods as well as a time-evolving block decimation (TEBD) algorithm [48]. We find that geometric frustration strongly enhances the photon repulsion on the lattice and leads to the emergence of a strongly correlated state of light, that we characterize by its incompressibility and crystalline order. Incompressibility is signaled by the appearance of an extended plateau in the average polariton excitation number as a function of drive strength, whose height is determined solely by the geometry of the lattice. Crystallization manifests itself in strong spatial photonic correlations, i.e., on-site and nearest-neighbor anti-bunching combined with extended density-wave oscillations at larger distances. Interestingly, we find that the correlation length of these oscillations can be increased when decreasing the light-matter coupling strength g with respect to the photon hopping rate J .

We study a variant of the driven dissipative JCH model, i.e.,

$$H = \sum_{j=1}^N \sum_{\alpha=A,B} h_{j\alpha} + J \sum_{j=1}^{N-1} \left[(a_j + a_{j+1}) b_j^\dagger + \text{H.c.} \right] \quad (1)$$

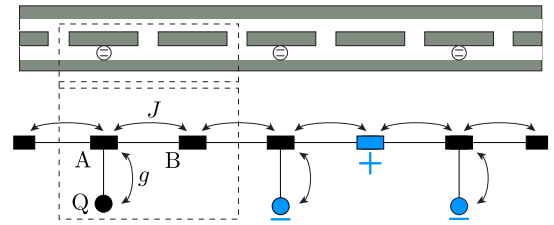


FIG. 1. Top panel: Sketch of a transmission line resonator chain including superconducting qubits in every other resonator. Bottom panel: Simplified lattice representation. Two cavities of type A and B (rectangles) are coupled by the photon hopping rate J . Qubits (circles) are only coupled to the A cavities with strength g . The dashed lines show one unit cell of the array and the blue symbols mark a localized plaquette state as discussed in the text (\pm denote the corresponding phases in the wavefunction), see Eq. (6).

where $h_{j,\alpha}$ denote the on-site Hamiltonians for resonators of type A and B with qubits at site Q coupling only to the A sites, i.e.,

$$\begin{aligned} h_{jA} &= \Delta_A a_j^\dagger a_j + \Delta_Q \sigma_j^+ \sigma_j^- + (g a_j^\dagger \sigma_j^- + f a_j + \text{H.c.}), \\ h_{jB} &= \Delta_B b_j^\dagger b_j + f (b_j + \text{H.c.}). \end{aligned} \quad (2)$$

Here, the bosonic operators a_j (b_j) annihilate a cavity photon at site A (B) in unit cell $j = 1, \dots, N$. The second term in (1) describes photon hopping to nearest neighbors at a rate J . The qubits are represented by Pauli operators σ_j^- and couple to the A photons with strength g . All cavities are subject to a coherent drive of strength f described by the last terms in (2). The Hamiltonian (1) is written in a frame rotating with the drive frequency ω_D such that the bare cavity and qubit frequencies ω_X are renormalized to $\Delta_X = \omega_X - \omega_D$, with $X = A, B, Q$.

Cavity dissipation is taken into account using a Lindblad master equation for the density matrix, i.e.,

$$\dot{\rho} = -i[H, \rho] + (\kappa/2) \sum_j (\mathcal{D}[a_j]\rho + \mathcal{D}[b_j]\rho), \quad (3)$$

with the Lindblad operator $\mathcal{D}[a]\rho = 2a\rho a^\dagger - a^\dagger a\rho - \rho a^\dagger a$ and the photon decay rate κ . Here, and in the following we neglect spontaneous emission and dephasing of the qubits, which can be substantially suppressed with respect to cavity decay [49]. Fig. 1 shows a possible implementation of our model based on state-of-the-art circuit QED technology [14]. A similar geometry can be realized using semiconductor micro-pillar arrays [17, 34].

We start with the discussion of the single-particle spectrum of (1) in the absence of drive ($f = 0$) and dissipation ($\kappa = 0$). For that purpose, we write a common Fourier transform $\psi_j = (1/\sqrt{N}) \sum_k e^{ikj} \psi_k$, with $\psi_j = [a_j, b_j, \sigma_j^-]^T$ and

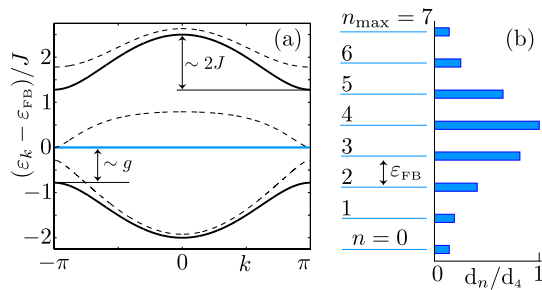


FIG. 2. (a) Single particle dispersion of the lattice shown in Fig. 1 with three bands. For $\delta_Q = J$ (dashed lines) all bands are dispersive. For $\delta_{QB} = \omega_Q - \omega_B = 0$ (solid lines) the middle band (blue) becomes flat corresponding to a set of degenerate single-particle plaquette states. (b) Many-body eigenstates associated with the flat band can be constructed from products of plaquettes (see discussion in the text). They form a bounded, equally spaced multi-level system indexed by the particle number $n = 0, \dots, n_{\max}$ with degeneracies $d_n = \binom{2n_{\max}-n}{n}$ and largest filling $n_{\max} = (N+1)/2$, which depends on the lattice size N . For example, the $n = 1$ level with degeneracy $d_1 = N$ corresponds to all states belonging to the single-particle flat band shown in (a). Here we show the case for $N = 13$ unit cells with $n_{\max} = 7$.

impose periodic boundary conditions. We then obtain the k -space representation of the lattice Hamiltonian, i.e.,

$$H = \sum_k \psi_k^\dagger \begin{bmatrix} \omega_A & J(1 + e^{-ik}) & g \\ J(1 + e^{ik}) & \omega_B & 0 \\ g & 0 & \omega_Q \end{bmatrix} \psi_k, \quad (4)$$

with $k = 2n\pi/N$, $n = -N/2, \dots, N/2 - 1$. The eigenvalue equation for (4) yields three bands, which are plotted in Fig. 2. For the general case with $\delta_{QB} = \omega_Q - \omega_B \neq 0$ all bands are dispersive (dashed lines). However, if $\delta_{QB} = 0$ the middle band turns flat while the other two remain dispersive with energies

$$\begin{aligned} \varepsilon_{FB} &= \omega_B, \\ \varepsilon_k^\pm &= \omega_B + \delta_{AB}/2 \pm \sqrt{2J^2(1 + \cos k) + g^2 + \delta_{AB}^2/4}, \end{aligned} \quad (5)$$

where $\delta_{AB} = \omega_A - \omega_B$. Note, that the flat band does not depend on δ_{AB}, g, J and is separated by a gap $\sqrt{g^2 + \delta_{AB}^2/4} \pm \delta_{AB}/2$ from the dispersive bands. The flat band eigenstates can be written as

$$|\Lambda_j\rangle = \frac{1}{\sqrt{g^2 + 2J^2}} [g b_j^\dagger - J(\sigma_j^+ + \sigma_{j+1}^+)] |\text{vac}\rangle, \quad (6)$$

which describes a localized plaquette defined by one B and two neighboring Q sites (see Fig. 1). The flat band arises due to the destructive interference between a photon hopping process from resonator B to A ($\sim J$) and the excitation transfer due to the coupling of Q to the resonator A ($\sim g$). As a consequence the A cavities remain completely dark, i.e., with vanishing photon amplitude, such that an excitation originally localized at one end of the chain does not disperse and/or propagate to the other end.

In the following, we are interested in the interplay of frustration and interactions in the non-equilibrium steady-state (NESS) of the system when all cavities are pumped coherently with strength f and dissipate photons with rate κ . The drive frequency is kept resonant with the flat band energy, i.e., $\omega_D = \varepsilon_{FB}$. In order to take into account states resonant with the drive, we construct from (6) the eigenstates of the Hamiltonian (1) (for vanishing drive amplitude, i.e., $f = 0$) with energies that are integer multiples of ε_{FB} , and project the full density matrix (3) on this subspace. Apart from the single-particle states in (6), these are states which are products of non-overlapping plaquettes, e.g., the two particle states $|\psi_2\rangle \sim |\Lambda_1\rangle |\Lambda_3\rangle, |\Lambda_1\rangle |\Lambda_4\rangle \dots$ with energy $2\varepsilon_{FB}$, the three particle states $|\psi_3\rangle \sim |\Lambda_1\rangle |\Lambda_3\rangle |\Lambda_5\rangle, |\Lambda_1\rangle |\Lambda_3\rangle |\Lambda_6\rangle \dots$ with energy $3\varepsilon_{FB}$ etc. The energetically highest lying state is the density-wave $|\Psi_{\text{dw}}\rangle = \prod_{j=1}^{n_{\max}} |\Lambda_{2j}\rangle$ with energy $\varepsilon_\Psi = n_{\max} \varepsilon_{FB}$ and particle number $n_{\max} = (N+1)/2$, i.e., filling per lattice site $\nu_\Psi = n_{\max}/(3N) = 1/6 + \mathcal{O}(1/N)$. This special ladder of flat band states is shown in Fig. 2 (b). It forms a set of $F_N = \sum_{n=0}^{n_{\max}} d_n$ equally spaced many-body levels with degeneracies $d_n = \binom{2n_{\max}-n}{n}$, where n is the particle number of each state. All eigenstates with a higher particle number $n > n_{\max}$ belong to dispersive bands and are gapped from the flat-band ladder due to the nonlinearity induced by the light-matter coupling g .

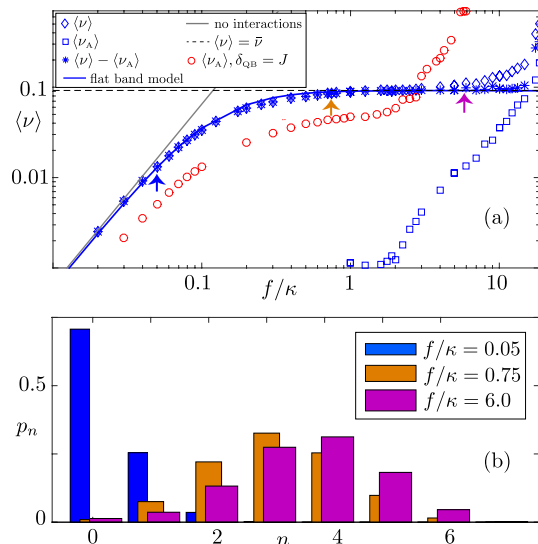


FIG. 3. (a) Average excitation number per lattice site $\langle \nu \rangle = \langle \nu_A \rangle + \langle \nu_B \rangle + \langle \nu_Q \rangle$, with $\nu_X = \sum_j x_j^\dagger x_j / 3N$, $X = A, B, Q$ and $x = a, b, \sigma^-$ respectively, as a function of pump strength f/κ . Shown are results as obtained from projection of the density matrix on the flat band eigenspace for a finite system with $N = 13$ unit cells (solid line) and from TEBD simulations of the infinite system at zero detuning $\delta_{QB} = 0$ (blue symbols) and finite detuning $\delta_{QB} = J$ (circles). Note, that the plateau is largely extended for the difference $\langle \nu \rangle - \langle \nu_A \rangle$ (asterisks) with a rather sharp departure from the plateau for strong pump. In the dispersive case with $\delta_{QB} \neq 0$ (the drive stays resonant with the bottom of the middle band) height and extent of the plateau are largely reduced. (b) Probability p_n of finding n excitations in the lattice as calculated within the flat band model for different pump strengths, which are marked with arrows in (a). For the TEBD simulations we used a local photon number cutoff of up to 3 photons in each cavity, the time step in the second-order Trotter decomposition is $dt = 0.05/J$ and the error due to matrix truncation is kept below 10^{-8} using bond dimensions up to 60. Other parameters: $g/J = 1$, $\delta_{AB}/J = 0.5$, $\kappa/J = 0.05$.

Due to the coherent drive with $\omega_D = \varepsilon_{FB}$ we expect states belonging to the flat band ladder to mostly contribute to the NESS at small and intermediate drive strength. In Fig. 3 we show the average excitation number per lattice site $\langle \nu \rangle$ (for a formal definition see caption of Fig. 3) as a function of relative pump strength f/κ calculated within the flat band projection model (solid blue line). At weak pump $f \ll \kappa$, the results of the projected model agree with the analytical expression $\langle \nu \rangle \approx (4f^2/\kappa^2)[1 + (4J^2 + \kappa^2/4)/g^2]$ (straight solid line), which is obtained from a perturbative calculation of the steady state to leading order in the drive strength f/κ . At stronger pump, however, the many-body states in the flat band ladder become progressively occupied until the system saturates at a filling $\langle \nu \rangle \approx \nu_\Psi/2$ resulting in an extended plateau centered around $f \sim \kappa$. This plateau can be interpreted as an incompressible state of photons with $\partial \langle \nu \rangle / \partial f \approx 0$, as we now explain in more detail. The height of the plateau is largely independent of g and J and determined only by the geometry of the lattice. This can be understood by looking at the excitation number distribution p_n of finding n excitations in the lat-

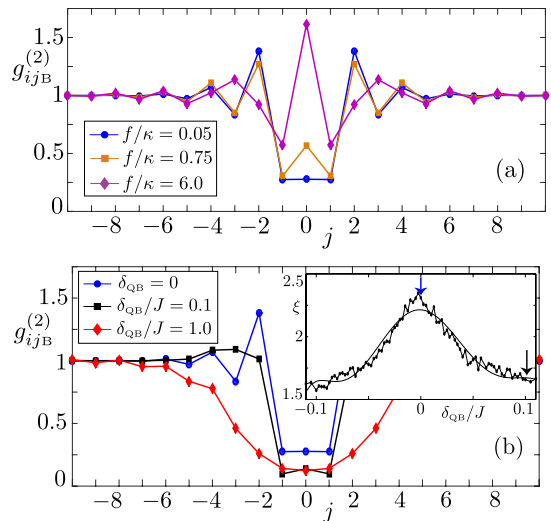


FIG. 4. Second-order coherence function of photons emitted by the B sites $g_{ijB}^{(2)} = \langle b_i^\dagger b_j^\dagger b_i b_j \rangle / \langle b_i^\dagger b_i \rangle \langle b_j^\dagger b_j \rangle$ for different drive strength's f/κ at zero detuning $\delta_{QB} = 0$ (upper panel) and detuning parameters δ_{QB}/J at drive strength $f/\kappa = 0.05$ (lower panel) as calculated with TEBD. In (b) the drive stays resonant with the bottom of the middle band (dispersive for $\delta_{QB} \neq 0$). The inset shows the length of the density-wave correlations ξ obtained from an exponential fit of the numerical data for small detunings $|\delta_{QB}|/J \leq 0.11$. Arrows mark the corresponding values in the main figure. Other parameters are chosen as in Fig. 3.

tice, shown in Fig. 3(b) as obtained from the projection model. At weak pumping the distribution is peaked at low excitation numbers and shifts to larger n for increasing pump strength. At strong pumping it saturates and resembles approximately the degeneracies d_n shown in Fig. 2(b), i.e., all states are almost equally occupied similar to a two-level system saturating half way between ground and excited state [50]. The peak position, i.e., the average excitation number is thus calculated as $\bar{n} \approx \sum_{n=0}^{n_{\max}} n d_n / F_N = (1 - 1/\sqrt{5})(N/2)$. This value corresponds to the horizontal dashed line in Fig. 3(a), which agrees with the height of the plateau in the saturated regime. Since $\bar{n} \approx n_{\max}/2$, we find the filling of the plateau at roughly half the density-wave filling $\bar{\nu} \approx \nu_\Psi/2 \approx 1/12$. Note, that the distribution saturates since many-particle states with filling higher than the density wave $\langle \nu \rangle > \nu_\Psi$ are gapped from the flat-band ladder due to effective photon repulsion as discussed earlier. The incompressible state thus originates from an unconventional photon blockade on a frustrated lattice arising from pumping an equally-spaced, degenerate multi-level system, i.e., the flat band ladder shown in Fig. 2(b).

We confirm this picture by employing an open system version of the time-evolving block decimation (TEBD) algorithm [48] (for technical details, see caption of Fig. 3). The average excitation number of the projected model agrees with the exact numerics (diamonds) well into the plateau, thus verifying the incompressible state of photons. Finally, for an even stronger pump ($f \gg \kappa$), the dispersive bands start to contribute to the NESS leading to a destruction of the incompressible state. This is also signaled by an increasing occupation of

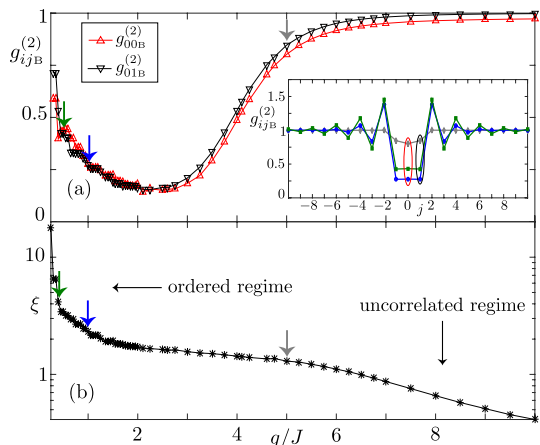


FIG. 5. (a) On-site and nearest-neighbor correlator $g_{00B}^{(2)}, g_{01B}^{(2)}$ as a function of the ratio g/J for a nominal weak drive strength $f/\kappa = 0.05$ (blue arrow in the upper panel of Fig. 3). The inset shows the complete spatial dependence of the correlator for $g/J = 0.5$ (squares), $g/J = 1$ (circles) and $g/J = 5$ (diamonds), as marked by the arrows in the main figure. (b) Correlation length as a function of g/J obtained from an exponential fit of the second-order coherence function. Other parameters are chosen as in Fig. 3.

the A-site cavities (squares) in Fig. 3(a). In this regime, the projected model becomes invalid and the full numerics very costly as the local Hilbert space cutoff needs to be increased substantially. The interesting details of this crossover are subject of future work.

We now investigate the spatial order of the steady state by studying the second-order coherence function (density-density correlator) of the B sites, i.e., $g_{ijB}^{(2)} = \langle b_i^\dagger b_j^\dagger b_i b_j \rangle / \langle b_i^\dagger b_i \rangle \langle b_j^\dagger b_j \rangle$. Fig. 4 shows the spatial correlations of the central site of the chain ($i = 0$) with its neighbors, as calculated with TEBD. At weak and intermediate strength f we find local ($j = 0$) as well as nearest neighbor ($j = \pm 1$) anti-bunching, which represent a signature of photon blockade and incompressibility, i.e., the resistance of the system to accept simultaneously two pump photons entering the chain either on the same or on neighboring plaquettes (which share a qubit, see Fig. 1). Thus, if a photon is present at the central site of the chain, every other B-site exhibits reduced occupation, i.e., remains darker due to effective photon-photon interactions, resulting in polaritonic density-wave like order. At larger distances, density-wave order manifests itself in spatial correlations which alternate between bunching ($g_{0(2j)B}^{(2)} > 1$) and anti-bunching ($g_{0(2j+1)B}^{(2)} < 1$) leading to a crystalline state of light. This can be interpreted as the non-equilibrium counterpart of a charge density wave appearing in the ground-state of an electronic or atomic system with a flat band as the energetically lowest band, e.g., in a sawtooth or Kagome lattice [29].

Under nominal weak pumping conditions, the spatial extent of the density-wave correlations depends sensitively on the ratio g/J , which also determines the photon/qubit nature of the plaquette states (see Eq. (6)). As shown in Fig. 5,

the correlation length vanishes when the flat band becomes photon-like, i.e., for $g \gg J$, while it diverges in the opposite limit ($g \ll J$), i.e., when the plaquette states (6) have a large qubit component. This can be understood by noting that the projection of the B photon operators on the flat band states, i.e., $b_j = \lambda^{-1}(|\text{vac}\rangle \langle \Lambda_j| + |\Lambda_j\rangle \langle \Lambda_{j+2}| + \dots)$ modifies the drive strength according to $f/\kappa \rightarrow \tilde{f}/\tilde{\kappa} = (f/\kappa)\lambda$, with $\lambda = \sqrt{1 + 2J^2/g^2}$. Thus, the drive strength effectively increases for the flat band when the light matter coupling strength g decreases with respect to the hopping rate J leading to a larger contribution to the NESS of the high-energy density-wave state $|\Psi_{\text{dw}}\rangle$ (with infinite correlation length). At the same time the gap to the other bands closes as $g \rightarrow 0$ leading to a destruction of the photon blockade effect. Consequently, we find the strongest anti-bunching roughly for the fully mixed polaritonic case with $g \sim \sqrt{2}J$.

Finally, we show that the signatures of geometric frustration, incompressibility and crystalline order vanish when the flat band becomes dispersive, i.e., when $\delta_{\text{QB}} \neq 0$ (the drive is kept resonant with the bottom of the band). For $\delta_{\text{QB}} = J$ (compare with the dashed lines in the spectra of Fig. 2), we observe in Fig. 3(a) that the extent of the excitation plateau shrinks by almost one order of magnitude. At the same time, density-wave like correlations at larger distances completely disappear and are replaced by a broad and rather featureless anti-bunching dip in Fig. 4(b), which was also predicted for regular 1D chains [4, 6]. Indeed, the correlation length of the density-wave oscillations drops quickly from its maximum flat band value to roughly the size of one unit cell (see inset of Fig. 4).

In summary, we have shown that geometric frustration in a photonic system leads to an incompressible and crystalline state of light with unique spatial ordering, i.e., local and nearest neighbour anti-bunching combined with density-wave correlations at larger distances. We have proposed a simple quasi-1D implementation of our model with superconducting qubits, which is realizable with state-of-the-art circuit QED technology and can be easily extended to two dimensions, e.g., to study topological effects. The onset of long-range correlations motivates another interesting question for future work, i.e., whether super-solid like behaviour of light (coexistence of superfluidity and density-wave order) could be observed for stronger pumping in a driven, dissipative flat band system (without the need of explicitly engineering nearest-neighbour interaction terms in the Hamiltonian [11, 51]). Our proposal thus paves the way for quantum simulations [52] of frustrated systems far from equilibrium and the realization of strongly correlated, exotic states of light with non-trivial spatial correlations.

We are grateful to A. Amo, F. Baboux, J. Bloch, C. Ciuti, K. LeHur, M. Bordyuh, H. E. Türeci and G. Zhu for fruitful discussions. We acknowledge financial support from the Swiss NSF through an Ambizione Fellowship (SS) under Grant No. PP00P2-123519/1 and the NCCR QSIT (MB).

-
- [1] A. D. Greentree, C. Tahan, J. H. Cole, and L. Hollenberg, *Nat. Phys.* **2**, 856 (2006).
- [2] M. Hartmann, F. Brandão, and M. Plenio, *Nat. Phys.* **2**, 849 (2006).
- [3] D. Angelakis, M. Santos, and S. Bose, *Phys. Rev. A* **76**, 031805 (2007).
- [4] I. Carusotto, D. Gerace, H. E. Türeci, S. De Liberato, C. Ciuti, and A. Imamoglu, *Phys. Rev. Lett.* **103**, 033601 (2009).
- [5] D. Gerace, H. E. Türeci, A. Imamoglu, V. Giovannetti, and R. Fazio, *Nat. Phys.* **5**, 281 (2009).
- [6] M. Hartmann, *Phys. Rev. Lett.* **104**, 113601 (2010).
- [7] S. Schmidt, D. Gerace, A. Houck, G. Blatter, and H. E. Türeci, *Phys. Rev. B* **82**, 100507 (2010).
- [8] F. Nissen, S. Schmidt, M. Biondi, G. Blatter, H. E. Türeci, and J. Keeling, *Phys. Rev. Lett.* **108**, 233603 (2012).
- [9] L. M. Sieberer, S. D. Huber, E. Altman, and S. Diehl, *Phys. Rev. Lett.* **110**, 195301 (2013).
- [10] A. Le Boité, G. Orso, and C. Ciuti, *Phys. Rev. Lett.* **110**, 233601 (2013).
- [11] J. Jin, D. Rossini, R. Fazio, M. Leib, and M. J. Hartmann, *Phys. Rev. Lett.* **110**, 163605 (2013).
- [12] J. Otterbach, M. Moos, D. Muth, and M. Fleischhauer, *Phys. Rev. Lett.* **111**, 113001 (2013).
- [13] A. A. Houck, H. E. Türeci, and J. Koch, *Nat. Phys.* **8**, 292 (2012).
- [14] S. Schmidt and J. Koch, *Annalen der Physik* **525**, 395 (2013).
- [15] K. M. Birnbaum, A. Boca, R. Miller, A. D. Boozer, T. E. Northup, and H. J. Kimble, *Nature* **436**, 87 (2005).
- [16] A. Reinhard, T. Volz, M. Winger, A. Badolato, K. J. Hennessy, E. L. Hu, and A. Imamoglu, *Nat. Phot.* **6**, 93 (2012).
- [17] I. Carusotto and C. Ciuti, *Rev. Mod. Phys.* **85**, 299 (2013).
- [18] C. Lang, D. Bozyigit, C. Eichler, L. Steffen, J. M. Fink, A. A. Abdumalikov, M. Baur, S. Philipp, M. P. da Silva, A. Blais, and A. Wallraff, *Phys. Rev. Lett.* **106**, 243601 (2011).
- [19] A. J. Hoffman, S. J. Srinivasan, S. Schmidt, L. Spietz, J. Aumentado, H. E. Türeci, and A. A. Houck, *Phys. Rev. Lett.* **107**, 053602 (2011).
- [20] C. Eichler, D. Bozyigit, C. Lang, L. Steffen, J. Fink, and A. Wallraff, *Phys. Rev. Lett.* **106**, 220503 (2011).
- [21] D. J. P. Morris, D. A. Tennant, S. A. Grigera, B. Klemke, C. Castelnovo, R. Moessner, C. Czternasty, M. Meissner, K. C. Rule, J.-U. Hoffmann, K. Kiefer, S. Gerischer, D. Slobinsky, and R. S. Perry, *Science* **326**, 411 (2009).
- [22] C. Nisoli, R. Moessner, and P. Schiffer, *Rev. Mod. Phys.* **85**, 1473 (2013).
- [23] T. Neupert, L. Santos, C. Chamon, and C. Mudry, *Phys. Rev. Lett.* **106**, 236804 (2011).
- [24] E. Tang, J.-W. Mei, and X.-G. Wen, *Phys. Rev. Lett.* **106**, 236802 (2011).
- [25] A. Petrescu, A. A. Houck, and K. Le Hur, *Phys. Rev. A* **86**, 053804 (2012).
- [26] M. Sigrist and T. M. Rice, *Rev. Mod. Phys.* **67**, 503 (1995).
- [27] M. V. Feigel'man, L. B. Ioffe, V. B. Geshkenbein, P. Dayal, and G. Blatter, *Phys. Rev. B* **70**, 224524 (2004).
- [28] C. Wu, D. Bergman, L. Balents, and S. Das Sarma, *Phys. Rev. Lett.* **99**, 070401 (2007).
- [29] S. D. Huber and E. Altman, *Phys. Rev. B* **82**, 184502 (2010).
- [30] M. Tovmasyan, E. P. L. van Nieuwenburg, and S. D. Huber, *Phys. Rev. B* **88**, 220510 (2013).
- [31] G. Zhu, J. Koch, and I. Martin, *ArXiv e-prints* (2014), arXiv:1411.0043 [cond-mat.mes-hall].
- [32] D. Tanese, H. Flayac, D. Solnyshkov, A. Amo, A. Lemaître, E. Galopin, R. Braive, P. Senellart, I. Sagnes, G. Malpuech, and J. Bloch, *Nat. Commun.* **4**, 1749 (2013).
- [33] M. Abbarchi, A. Amo, V. G. Sala, D. D. Solnyshkov, H. Flayac, L. Ferrier, I. Sagnes, E. Galopin, A. Lemaître, G. Malpuech, and J. Bloch, *Nat. Phys.* **9**, 275 (2013).
- [34] T. Jacqmin, I. Carusotto, I. Sagnes, M. Abbarchi, D. D. Solnyshkov, G. Malpuech, E. Galopin, A. Lemaître, J. Bloch, and A. Amo, *Phys. Rev. Lett.* **112**, 116402 (2014).
- [35] J. Raftery, D. Sadri, S. Schmidt, H. Tureci, and A. Houck, *Phys. Rev. X* **4**, 031043 (2014).
- [36] C. Eichler, Y. Salathe, J. Mlynek, S. Schmidt, and A. Wallraff, *Phys. Rev. Lett.* **113**, 110502 (2014).
- [37] M. Aichhorn, M. Hohenadler, C. Tahan, and P. Littlewood, *Phys. Rev. Lett.* **100**, 216401 (2008).
- [38] M. Knap, E. Arrighoni, and W. von der Linden, *Phys. Rev. B* **81**, 104303 (2010).
- [39] M. Hohenadler, M. Aichhorn, S. Schmidt, and L. Pollet, *Phys. Rev. A* **84**, 041608(R) (2011).
- [40] M. Hohenadler, M. Aichhorn, L. Pollet, and S. Schmidt, *Phys. Rev. A* **85**, 013810 (2012).
- [41] S. Schmidt and G. Blatter, *Phys. Rev. Lett.* **103**, 086403 (2009).
- [42] J. Koch and K. L. Hur, *Phys. Rev. A* **80**, 023811 (2009).
- [43] S. Schmidt and G. Blatter, *Phys. Rev. Lett.* **104**, 216402 (2010).
- [44] T. Grujic, S. R. Clark, D. Jaksch, and D. G. Angelakis, *New J. Phys.* **14**, 103025 (2012).
- [45] S. Schmidt, G. Blatter, and J. Keeling, *J. Phys. B* **46**, 224020 (2013).
- [46] G. Zhu, S. Schmidt, and J. Koch, *New J. Phys.* **15**, 115002 (2013).
- [47] D. Guzmán-Silva, C. Mejía-Cortès, M. A. Bandres, M. C. Rechtsman, S. Weimann, S. Nolte, M. Segev, A. Szameit, and R. A. Vicencio, *New J. Phys.* **16**, 063061 (2014).
- [48] M. Zwolak and G. Vidal, *Phys. Rev. Lett.* **93**, 207205 (2004).
- [49] J. Koch, T. Yu, J. Gambetta, A. Houck, D. Schuster, J. Majer, A. Blais, M. Devoret, S. Girvin, and R. Schoelkopf, *Phys. Rev. A* **76**, 042319 (2007).
- [50] L. Bishop, J. M. Chow, J. Koch, A. A. Houck, M. H. Devoret, E. Thuneberg, S. M. Girvin, and R. J. Schoelkopf, *Nat. Phys.* **5**, 105 (2009).
- [51] A. van Otterlo, K.-H. Wagenblast, R. Baltin, C. Bruder, R. Fazio, and G. Schön, *Phys. Rev. B* **52**, 16176 (1995).
- [52] I. M. Georgescu, S. Ashhab, and F. Nori, *Rev. Mod. Phys.* **86**, 153 (2014).